ACS OMEGA

http://pubs.acs.org/journal/acsodf

Article

TMT-Based Proteomics Analysis of the Intervention Effect of Orlistat on Polycystic Ovary Syndrome Rats Induced by Letrozole Combined with a High-Fat Diet

Jianmei Yang, Enli Wang, Wenbin Chen, Baihui Xu, Chen Chen, Guimin Zhang,* and Jingchun Yao*

Cite This: *ACS Omega* 2023, 8, 24831−24840

Read Online

ACCESS | Metrics & More | Article Recommendations | Supporting Information

ABSTRACT: Polycystic ovary syndrome (PCOS) is a complex gynecological endocrine and metabolic disease. Orlistat as a lipase inhibitor may improve the pathological characteristics of PCOS and is the sole antiobesity agent available in various countries. In this study, the PCOS rat models were established using letrozole and high-fat diet. Tandem Mass Tag labeling peptide coupled with liquid chromatography with tandem mass spectrometry (LC-MS/MS) approach was employed to investigate the differentially expressed ovarian proteins (DEPs) in the PCOS and control rats for the effect of PCOS, and in the PCOS and orlistat-treated PCOS rats for the effect of orlistat in PCOS. The orlistat attenuated the body weight gain; decreased the levels of testosterone, luteinizing hormone, a ratio of luteinizing/follicle-stimulating hormones; increased the level of estradiol; and recovered the estrous cycle in PCOS rats. In addition, 795 and 119 DEPs were found in PCOS and orlistat-treated PCOS groups, respectively. Based on the Gene Ontology and Kyoto Encyclopedia of Gene and Genomes pathway analysis of DEPs, orlistat restored the disturbed metabolism of linoleic acid, arachidonic acid, galactose, and glycerolipids, and then improved the chronic inflammation in PCOS rats. This study analyzed the ovarian proteome of orlistat-treated PCOS rats and identified targeted proteins, which explored the pathogenesis of PCOS and the potential effects of orlistat in PCOS rats.

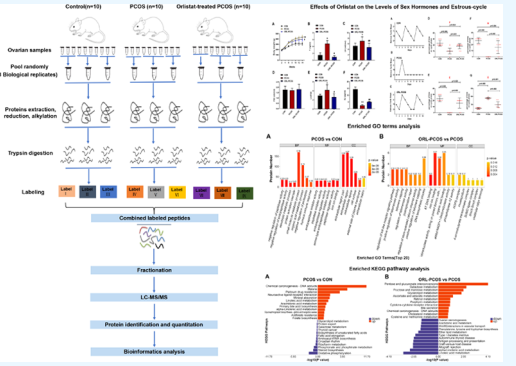

1. INTRODUCTION

Polycystic ovary syndrome (PCOS) is a complex gynecological endocrine and metabolic disease with a prevalence rate of 8−13% according to the population studied and the definitions used.[1] PCOS is characterized by hyperandrogenemia, infertility, and ovarian dysfunction and is associated with metabolic consequences, including insulin resistance (IR), type 2 diabetes (T2DM), and obesity.[2] Although the clinical experience is considerable, the pathophysiology and molecular basis of PCOS are not fully understood because of its heterogeneity and complexity.[3]

Proteomics is an efficient and powerful method to investigate complex biological processes.[4] Previous relevant findings have been discovered in proteomic studies of PCOS, providing much valuable information about the pathophysiology of PCOS. Recently, Sim et al. performed a comparative proteomic analysis of human follicular fluid (FF) from PCOS and non-PCOS patients using two-dimensional gel electrophoresis (2-DE) combined with mass spectrometry (MS). Seven differentially expressed proteins (DEPs) were identified, which may serve as potential pathological biomarkers during oocyte development.[5] In addition, several proteins in serum samples, such as haptoglobin, fibrinogen, and lipoprotein lipase, have been identified by MS with isobaric tags for relative and absolute quantification (iTRAQ) as candidate biomarkers in predicting the development of ovarian hyperstimulation syndrome among PCOS patients.[6] Another tandem mass tag (TMT)-based proteomics and bioinformatics analysis identified 70 DEPs in FF samples between infertile patients with or without PCOS and found that the inflammatory response, regulation of protein metabolic processes, and lipid transport were deregulated in PCOS, which played important roles in the pathogenesis of PCOS.[7] These newly discovered proteins may be involved in the pathogenesis of PCOS, but it is still a challenge to identify proteins that may lead to PCOS development.

Over 50% of women with PCOS are overweight or obese.[8] Evidence implies that obesity worsens infertility, hyperandrogenemia, metabolism, and IR in PCOS patients.[9] Weight loss, which may improve pregnancy outcomes and endocrine disorders in obese PCOS patients, is the first-line treatment for overweight women with PCOS.[10] The lipase inhibitor orlistat was found to improve or reverse the pathological character-

Received: January 28, 2023
Accepted: June 20, 2023
Published: June 29, 2023

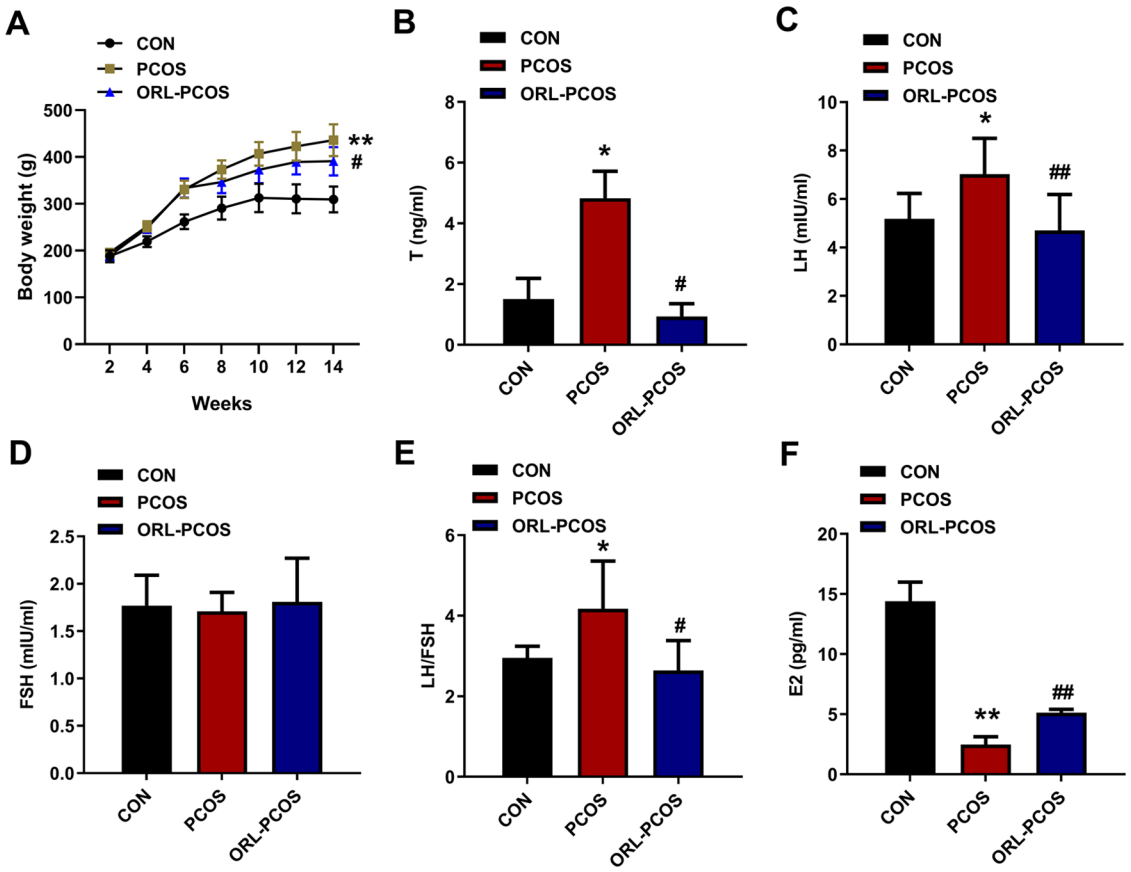

Figure 1. Effect of orlistat treatment on body weight and serum sex hormone levels in letrozole-induced PCOS rats. (A) Changes in body weight of rats in each group (0−2 weeks was the adaptation period, 2−6 weeks was the letrozole-induced PCOS rat period, and 6−14 weeks was the orlistat treatment period). (B) T, (C) LH, (D) FSH, (E) LH/FSH, (F) E2. All values represent mean ± SD (n = 10/group). *p < 0.05, **p < 0.01 vs CON; #p < 0.05, ##p < 0.01 vs PCOS. CON: control; PCOS: polycystic ovary syndrome; ORL-PCOS: orlistat-treated PCOS; T: testosterone; LH: luteinizing hormone; FSH: follicle-stimulating hormone; E2: estradiol.

istics of PCOS patients and became the sole antiobesity agent available in various countries.[11] Kumar et al. found that orlistat was as effective as metformin in weight loss by improving the lipid profile and pregnancy rates in PCOS women.[12] Moreover, several studies have shown that reduced testosterone levels were associated with orlistat administration.[12,13] Only a small amount of research on the mechanism of orlistat for the improvement in PCOS has been conducted, especially with regard to the proteome. In the present study, the effects of orlistat on PCOS rats induced by high-fat diet and letrozole, a nonsteroidal aromatase inhibitor widely used in PCOS modeling, were carefully examined.[14,15] A TMT-based liquid chromatography−tandem mass spectrometry (LC-MS/MS) was employed to investigate the ovarian tissue proteomic changes between PCOS rats (PCOS group) and orlistat-treated PCOS rats (ORL-PCOS group), in order to better understand the underlying effect of orlistat on PCOS.

2. RESULTS

2.1. Effects of Orlistat on Body Weight, Levels of Sex Hormones, and Estrous Cycle. To gain insight into the possible mechanisms, we constructed a PCOS rat model and used orlistat as a therapeutic intervention. In this study, after letrozole treatment and high-fat diet, the rats exhibited irregular estrous cycles, increased weight gain, increased circulating T and LH concentrations, and decreased level of serum E2, demonstrating that PCOS modeling was successful. As shown in Figure 1A, rats in the PCOS group exhibited a remarkable weight gain compared to those in the CON group (p < 0.01), while treatment with orlistat effectively reduced the increased body weight (p < 0.05) in PCOS. Additionally, the levels of various sex hormones in the serum from the different groups were determined. Compared with those of the CON group, the levels of serum T, LH, and the ratio of LH/FSH were significantly higher (p < 0.05; Figure 1B,C,E), and the level of serum E2 was significantly lower (p < 0.01; Figure 1F) in the PCOS group. The rats in the orlistat-PCOS group had significantly lower levels of T (p < 0.05; Figure 1B), LH (p < 0.01; Figure 1C), and the ratio of LH/FSH (p < 0.05; Figure 1E) and higher levels of E2 (p < 0.01; Figure 1F) than those of the rats in PCOS group without orlistat treatment. No differences were found in the FSH levels in the PCOS vs CON group and ORL-PCOS vs PCOS group (Figure 1D).

Estrous cycle assessment revealed that PCOS rats experienced a longer diestrus, shorter proestrus, and estrus than those of control rats (Figure 2A,B,D−G). Following orlistat treatment, the estrous cycle disorder was partially restored (Figure 2C,D−G).

2.2. Quantitative Overview of the Identified Proteins. In this study, proteins identified in at least three replicates with fold changes >1.2 or <1/1.2 and p < 0.05 were considered as DEPs. Volcano plots were mapped to show significant differences based on the fold change and p value in the PCOS vs CON group (Figure 3A) and ORL-PCOS vs PCOS

https://doi.org/10.1021/acsomega.3c00578
ACS Omega 2023, 8, 24831−24840

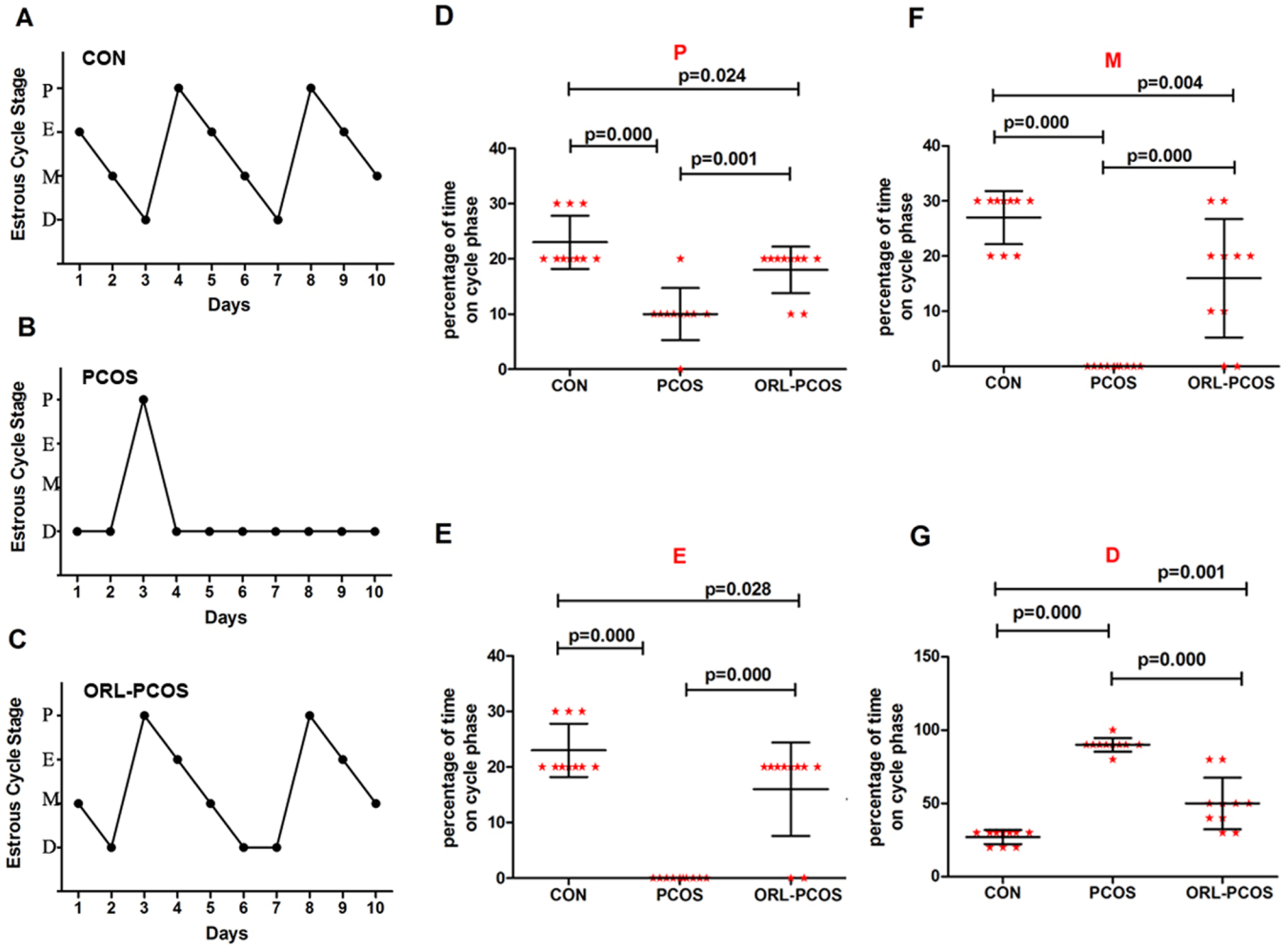

Figure 2. (A–C) Changes of estrous cycle of rats in CON, PCOS, and ORL-PCOS groups. (D–G) Relative time span of each stage of the cycle. P: proestrus; E: estrus; M: metestrus; D: diestrus; CON: control; PCOS: polycystic ovary syndrome; ORL-PCOS: orlistat-treated PCOS.

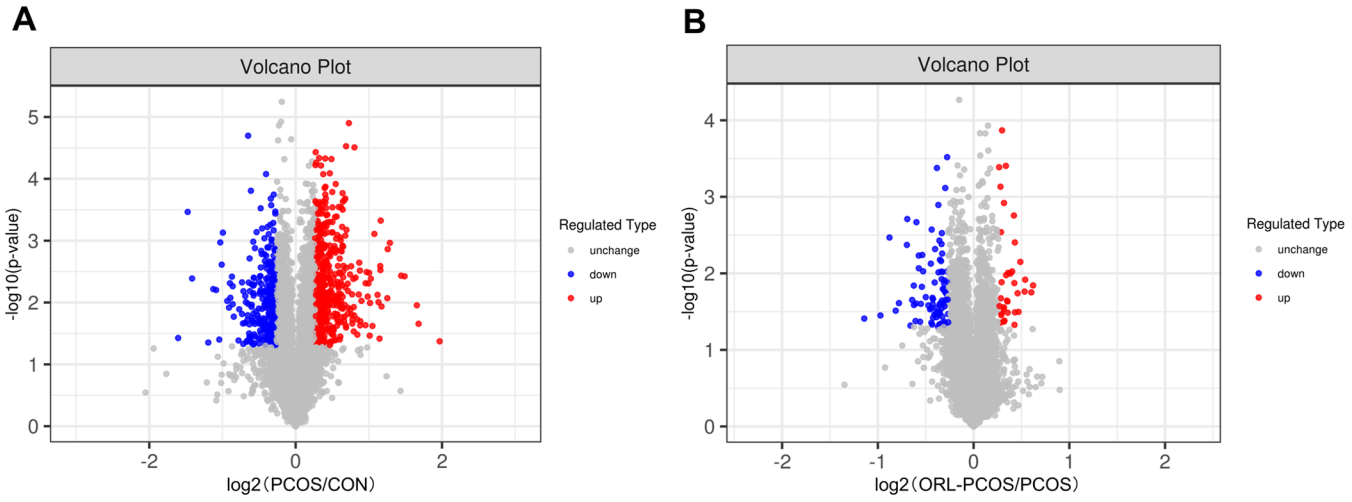

Figure 3. (A) Volcano plot of proteins identified from PCOS vs CON group. (B) Volcano plot of proteins identified from ORL-PCOS vs PCOS group. The volcano plot was mapped on the basis of the fold change and *p* values. Red and blue dots: DEPs; gray dots: proteins without difference; DEPs: differentially expressed proteins; CON: control; PCOS: polycystic ovary syndrome; ORL-PCOS: orlistat-treated PCOS.

group (Figure 3B). Compared with the CON group, 490 and 305 proteins were upregulated and downregulated in the PCOS group, respectively. Compared with the PCOS group, 35 and 84 proteins were upregulated and downregulated in the ORL-PCOS group, respectively. Detailed information on the DEPs is listed in Tables S1 and S2.

2.3. GO Enrichment Analysis of the DEPs. GO enrichment analysis of three distinctive functional sets, namely,

https://doi.org/10.1021/acsomega.3c00578
ACS Omega 2023, 8, 24831−24840

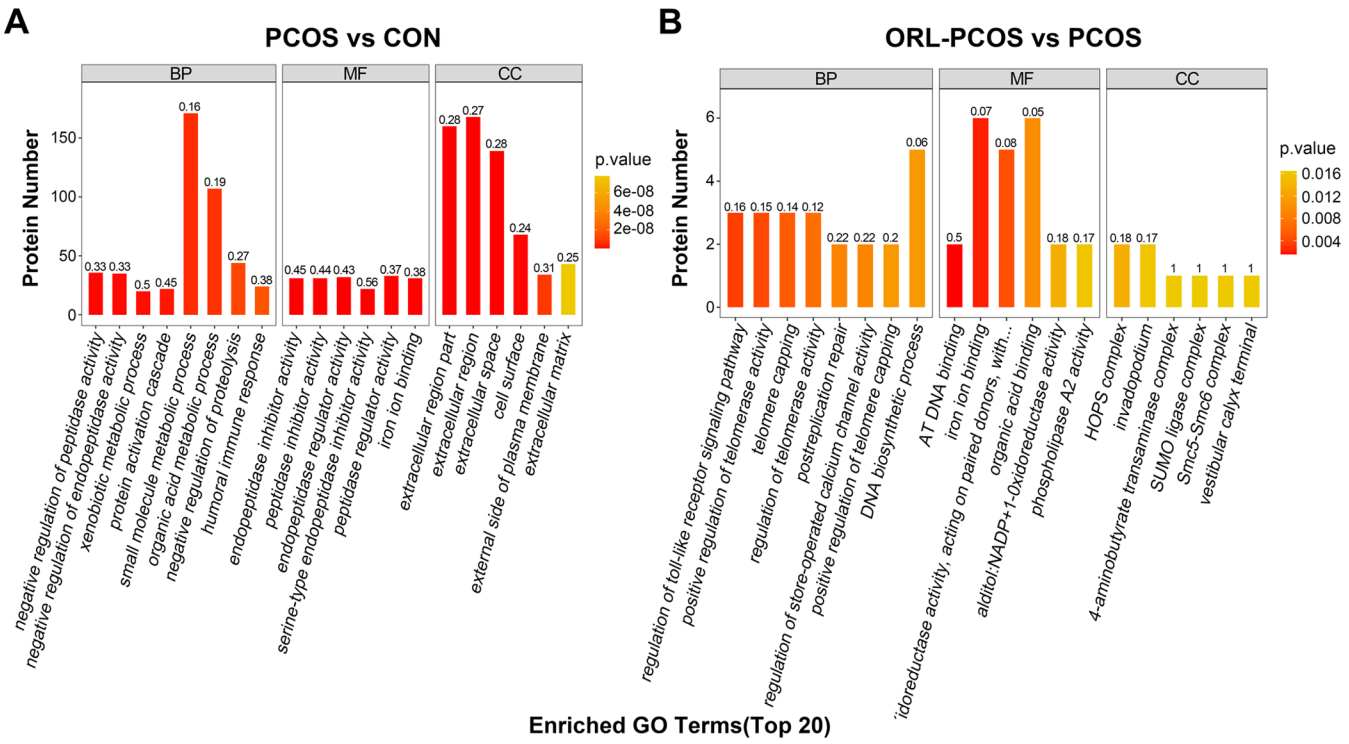

Figure 4. Enriched GO terms of the DEPs. (A) GO enrichment of the DEPs in PCOS vs CON group. (B) GO enrichment of the DEPs in ORL-PCOS vs PCOS group. GO: Gene Ontology; DEPs: differentially expressed proteins; CON: control; PCOS: polycystic ovary syndrome; ORL-PCOS: orlistat-treated PCOS; CC: cellular component; MF: molecular function; BP: biological process.

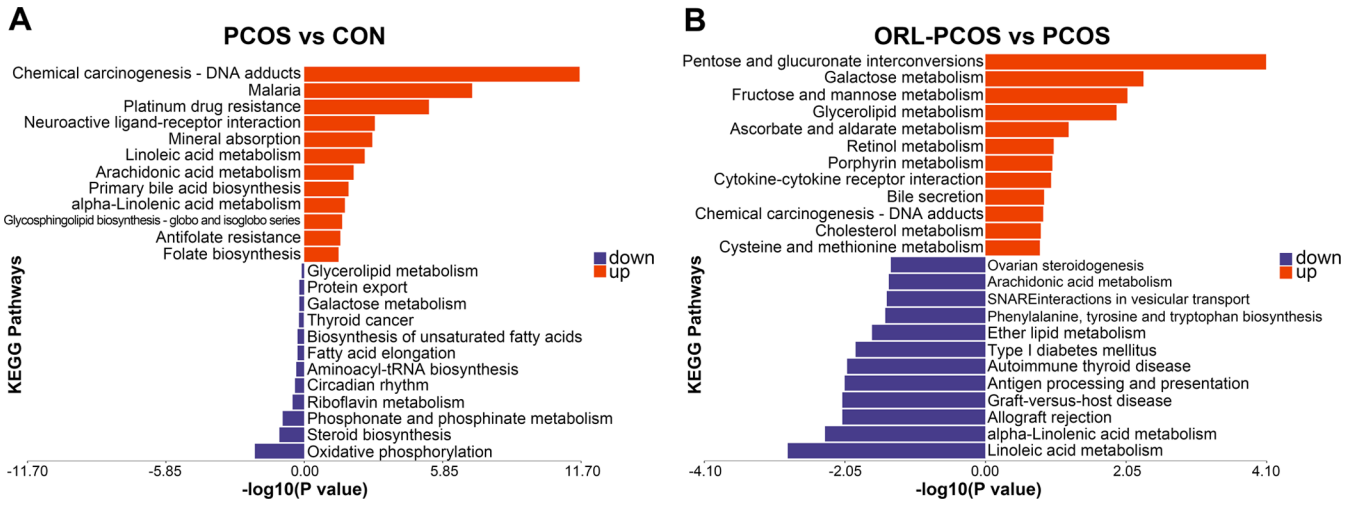

Figure 5. Enriched KEGG pathway analysis of the DEPs. (A) KEGG pathway analysis of the DEPs in PCOS vs CON group. (B) KEGG pathway analysis of the DEPs in ORL-PCOS vs PCOS group. KEGG: Kyoto Encyclopedia of Gene and Genomes; DEPs: differentially expressed proteins; CON: control; PCOS: polycystic ovary syndrome; ORL-PCOS: orlistat-treated PCOS.

cellular component (CC), molecular function (MF), and biological process (BP), was applied with a corrected statistically significant level ($p < 0.05$). In the BP category, DEPs in the PCOS vs CON group were primarily related to small-molecule metabolic processes and organic acid metabolic processes (Figure 4A). DEPs in the ORL-PCOS vs PCOS group were primarily related to DNA biosynthetic processes and regulation of the Toll-like receptor signaling pathways (Figure 4B). In terms of MF, DEPs in these two groups were mainly involved in iron ion bindings.

2.4. KEGG Pathway Analysis of the DEPs. According to the KEGG pathway enrichment analysis (Figure 5A), the upregulated proteins in the PCOS vs CON group were mainly involved in chemical carcinogenesis-DNA adducts, linoleic acid metabolism, and arachidonic acid metabolism, and the pathways associated with downregulated proteins were related to oxidative phosphorylation, steroid biosynthesis, and galactose and galactose metabolism. After orlistat treatment, the upregulated proteins in the ORL-PCOS vs PCOS group were mainly involved in galactose and galactose metabolism, and pentose and glucuronate interconversions, and the pathways associated with downregulated proteins were related to linoleic acid metabolism, arachidonic acid metabolism, and type 1 diabetes mellitus (Figure 5B).

https://doi.org/10.1021/acsomega.3c00578
ACS Omega 2023, 8, 24831−24840

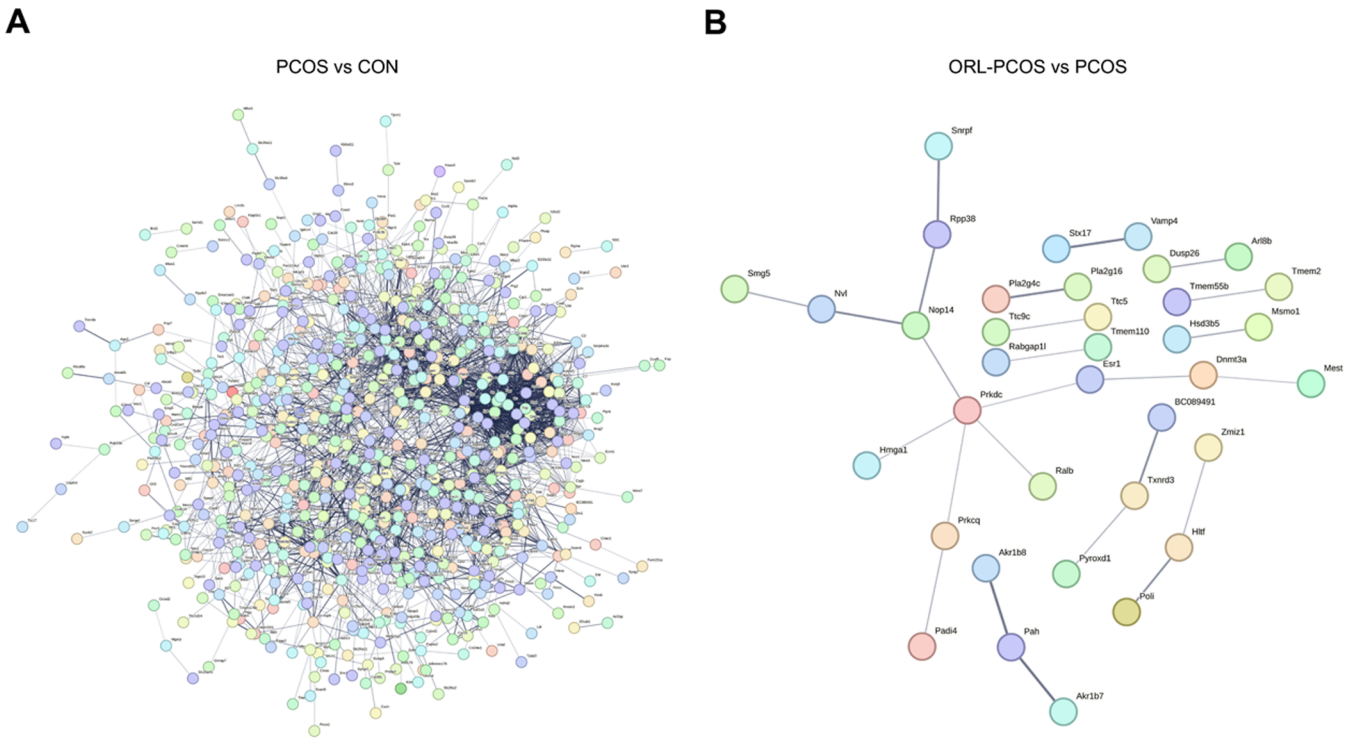

Figure 6. Protein−protein interaction (PPI) network based on DEPs. (A) PCOS vs CON group. (B) ORL-PCOS vs PCOS group. DEPs: differentially expressed proteins; CON: control; PCOS: polycystic ovary syndrome; ORL-PCOS: orlistat-treated PCOS.

2.5. Protein−Protein Interaction (PPI) Analysis. To understand how all of these DEPs were related and how they were involved in different biological networks that cross-link to each other, a PPI network was constructed from STRING database. DEPs that connected higher than others in the created network were considered as hub proteins (Figure 6). These hub proteins might have significant roles in the regulation of the network. There were many hub proteins in the PCOS vs CON group PPI network, but in the ORL-PCOS group PPI network, only a few hub proteins were found, such as Prkdc and Nop14.

3. DISCUSSION

Lipid metabolism disorders, such as obesity and hyperlipidemia, are common in PCOS cases.[16] Lipids are involved in various metabolic pathways, such as steroid hormone biosynthesis and fatty acid metabolism.[17] Orlistat significantly improves the lipid profile, including a significant decrease in total cholesterol, low-density lipoprotein (LDL), and triglycerides in PCOS women.[12] In this study, based on the KEGG enrichment analysis, the ORL-PCOS vs PCOS group had more DEPs involved in linoleic acid (LA) metabolism and arachidonic acid (AA) metabolism, including phospholipase A2 group IVC (PLA2G4C), phospholipase A2 group IIA (PLA2G2A), and phospholipase A and acyltransferase 3 (PLAAT3). PLA2G4 and PLA2G2A belong to the phospholipase A2 (PLA2) family, whose common function is to hydrolyze the fatty acids, playing pivotal roles in cell signaling and inflammation.[18] PLA2G4 is specific for the cleavage of AA from the second position of membrane phospholipids, while PLA2G2A hydrolyzes any fatty acid in the second position.[19] A previous study found that the mRNA expression levels of PLA2G2A and the protein expression levels of PLA2G4 were higher in the ovarian tissues of PCOS rats, and the production of AA was decreased via PLA2G4 catalysis, resulting in lower concentrations of polyunsaturated fatty acids (PUFAs) (LA and AA) in the ovarian tissues of PCOS rats than in controls.[20] PUFAs are the most effective fatty acid regulators in metabolic function. For example, n-3 PUFAs may effectively improve hyperandrogenism and IR in PCOS patients.[21] In addition, PLA2G4 was reported to regulate uterine prostaglandin (PG) production.[22] PGs, as lipid mediators, play important roles in chronic inflammation and the development of many reproductive events, disturbances of them are the characteristics of PCOS.[23] It was shown that the levels of PGs (PGD2, PGE2 PGI2, and PGF2α) were significantly higher in the ovarian tissues of PCOS rats than in those of healthy controls.[20] Consistent with a previous study, the upregulation of PLA2G4 and PLA2G2A was confirmed in the PCOS vs CON group, but the downregulation of PLA2G4 and PLA2G2A was observed in the ORL-PCOS vs PCOS group, suggesting that orlistat restored the lipid metabolism disorders, improved the levels of PUFAs, and decreased the levels of PGs in ovarian tissues of the PCOS by inhibiting the expression of these two proteins. Another protein that is involved in LA metabolism is PLAAT3, which plays a pivotal role in regulating the lipid storage of adipocytes.[24] Suppression of PLAAT3 expression significantly reduced the adipocyte-related gene expression and lipid accumulation in 3T3-L1 cells.[25] Jaworski et al. showed that the PLAAT3-deficient mice fed a high-fat diet had a slower weight gain than wild-type mice, and significantly smaller adipocytes in size and lower level of triacylglycerol.[26] Moreover, the amount of adipose prostaglandin E2 (PGE2) in PLAAT3-deficient mice was markedly reduced.[26] PGE2 was shown to promote adiposity in mice through inhibition of lipolysis.[27] Very recently, it was reported that the level of PGE2 in FF was negatively correlated with the high-quality embryo rate in PCOS patients.[28] Therefore, we

https://doi.org/10.1021/acsomega.3c00578
ACS Omega 2023, 8, 24831−24840

speculated that PLAAT3 might be an important effective target of orlistat on weight control and visceral white adipose tissue loss.

In the KEGG pathway enrichment analysis, we found that aldo-keto reductase family 1, member B7 (AKR1B7), aldo-keto reductase family 1, member B8 (AKR1B8), UDP glucuronosyltransferase 2 family, and polypeptide B10 (Ugt2b10) were enriched in pentose and glucuronate interconversions, which was the most significantly upregulated pathway in the ORL-PCOS vs PCOS group. AKR1B8 is the structurally and functionally closest related protein of AKR1B7.[29] AKR1B7 is a member of the aldo-keto reductases, which are NADPH-dependent oxidoreductases that convert aldehydes and ketones to primary and secondary alcohols, respectively.[30] AKR1B7 is expressed in a restricted set of tissues, such as adrenal glands, intestine, reproductive organs, and liver.[31] AKR1B7 is a main regulator of white adipose tissue development. In 3T3-L1 preadipocytes, AKR1B7 overexpression inhibited their differentiation, while knockout of AKR1B7 accelerated the adipogenesis process.[32] Moreover, the enrichment of AKR1B7 in the adipose stromal fraction plays a key role in preventing obesity in vivo by controlling the content of PGF2α. Compared with a standard diet, an aggravated obesity phenotype was observed in AKR1B7 knockout mice fed with an HFD, accompanied by a significant increase in the plasma levels of triglycerides, glycerol, and free fatty acids. Hence, a lack of AKR1B7 causes severe overweight.[27] In addition, the expression of AKR1B7 in the liver significantly reduces hepatic lipid accumulation and lowers blood glucose levels in diabetic mice, suggesting that AKR1B7 may be a therapeutic target for the treatment of fatty liver disease related to diabetes.[33] A previous study also demonstrated a high level of AKR1B7 expression in ovarian theca cells after human chorionic gonadotropin (hCG) treatment, suggesting its important role in ovulatory processes.[34] However, another study reported that AKR1B7 expression was dispensable for ovarian function. The estrous cycle and follicle maturation appeared normal, while progesterone was decreased during estrous in AKR1B7 knockout mice.[35] In this current study, the estrous cycle in the PCOS group basically stopped and most of them were in the diestrus period, which was consistent with previous studies. Guo et al. found that the PCOS rats induced by letrozole were constantly in the diestrus stage.[36] Wu et al. also found that compared to normal rats, most of the PCOS rats induced by letrozole were in the diestrus phase.[37] Following orlistat treatment, the estrous cycle disorder was partially restored. Orlistat significantly increased the expression of AKR1B7, which was reduced in PCOS rat ovaries. The human ortholog of mouse AKR1B7 is AKR1B10, which shares 89% amino acid homology with the mouse AKR1B7.[33] It would be interesting to explore whether human AKR1B10 is involved in the pathogenesis of PCOS, such as menstrual cycle disturbance, and whether it may serve as a therapeutic target for orlistat in the treatment of PCOS.

Previous proteomics studies have demonstrated that DEPs in PCOS ovaries are involved in the immune response and low-grade chronic inflammation, which is a key contributor to the PCOS pathogenesis and affects the occurrence of IR and ovarian dysfunction.[38] Inflammation may also affect important physiological processes that ultimately lead to infertility in PCOS patients.[39] In the current study, according to the GO enrichment analysis, the ORL-PCOS vs PCOS group had a lower abundance of proteins involved in the regulation of the Toll-like receptor signaling pathways, such as lipopolysaccharide-binding protein (LBP). LBP, one of the most important ligands of lipopolysaccharide (LPS), transfers LPS to the LPS receptor, ultimately resulting in the activation of TLR4 and inflammatory pathways.[40] In addition, serum LBP levels are positively correlated with several metabolic disorders, including obesity, IR, and T2DM.[41] Studies have also indicated the potentially important roles of LBP in the pathogenesis of PCOS. For example, Banaszewska et al. revealed that serum LBP levels were significantly elevated in PCOS women compared to healthy controls and were positively correlated with free testosterone and total cholesterol.[42] Similarly, Zhu et al. also found that serum LBP levels were significantly increased and associated with IR in women with PCOS.[40] Additionally, it was demonstrated that orlistat treatment decreased the plasma LBP level by 16.9% compared with that in high-fat- and high-cholesterol-induced obese hamsters, and significantly suppressed the increase in IL-6 and CD14 in hamsters.[43] Consistent with previous findings, the ovarian LBP levels were upregulated (1.57-fold) in PCOS rats and downregulated (0.77-fold) after orlistat intervention, suggesting that orlistat might attenuate the low-grade chronic inflammation state of PCOS by reducing LBP expression.

4. CONCLUSIONS

This study provides a comprehensive analysis of the differentially expressed ovarian proteins in the PCOS vs CON group and the ORL-PCOS vs PCOS group employing TMT-based quantitative proteomics. Orlistat may restore the PCOS-associated disorders in linoleic acid and arachidonic acid metabolism, and galactose and glycerolipid metabolism, as well as improve the chronic inflammation state of PCOS rats. PLA2G4, PLA2G2A, PLAAT3, AKR1B7, and LBP may be correlated with the pathogenesis of PCOS and may be used as therapeutic targets of orlistat in the treatment of PCOS. Despite the above significant achievement, this study does have several limitations, such as the limited sample size and lack of detailed validations. Further study is warranted to explore fully the clinical implication of the experimental results from this report

5. MATERIALS AND METHODS

This study was performed in accordance with the ethical standards specified in the Declaration of Helsinki, and the Medical Ethics Committee of Lunan Pharmaceutical Group Co., Ltd. approved all procedures (Permit No. AN-IACUC-2021-067).

5.1. Animals. Thirty-five specific pathogen-free female rats (5−6 weeks, 145−165 g, Animal Qualification Certificate No. 370726211100731686) were purchased from Beijing Vital River Laboratory Animal Technology Co., Ltd. (Certificate No. SCXK, 2016-0006; Beijing, China). Before the experiment, all of the rats were fed adaptively and quarantined for 2 weeks. Rats were housed in a breeding room under standard conditions (20−26 °C, 40−70% relative humidity, centralized ventilation of central air conditioner ≥15 times per hour, 12 h dark/light cycle). During the experiment, 10 rats were randomly selected as a control group (CON) and were fed a high-fat diet with 45% of kcal from fat (OpenSource Diets Research Diets #D12451). The other 25 rats were free to drink water and fed with a high-fat diet with 45% of kcal from fat combined with letrozole (1 mg/kg/day, Jiangsu Hengrui

https://doi.org/10.1021/acsomega.3c00578
ACS Omega 2023, 8, 24831−24840

Pharmaceutical Co., Ltd; Jiangsu, China) for 28 days to generate a PCOS model.[37] Vaginal epithelial cell smears were taken daily for 10 consecutive days to analyze the estrous cycle stage. The selection criteria for successfully inducing PCOS rats were referred to that of Kafali et al.[15] Twenty-three of 25 rats were identified as successfully induced PCOS rats. Then, 20 letrozole successfully induced PCOS rats were randomly selected and divided into two groups (n = 10/group). Ten rats were randomly selected as a PCOS control group (PCOS). The remaining 10 rats were then additionally supplemented with orlistat (80 mg/kg/day, Lunan Pharmaceutical Group Corporation; Shandong, Linyi, China) for the next 8 weeks. The dose of orlistat was selected based on a previous study.[44] Letrozole was given throughout the experiment to the PCOS rats. The control group and PCOS group were given the same volume of solvent without orlistat. Orlistat or solvent was administered by oral gavage.

5.2. Sample Collection. After orlistat treatment, the rats were weighed every week. Rats in each group were fasted for 24 h after the last administration. Blood was taken from the abdominal aorta to sacrifice the rats. Blood samples were collected and then centrifuged at 4000 rpm for 10 min at 4 °C. The levels of serum sex hormones, including testosterone (T), estradiol (E2), follicle-stimulating hormone (FSH), and luteinizing hormone (LH), were tested using radioimmunoassay (Beijing North Institute of Biotechnology Co., Ltd. Beijing, China) according to the specifications for each kit. The bar plots in this study were generated with GraphPad Prism 8.0 (GraphPad Software, San Diego). Data were analyzed with SPSS 18.0 (IBM SPSS, Armonk, NY) using the Mann−Whitney U test and are expressed as mean ± standard deviation (SD). A p value of <0.05 was considered statistically significant. After exposing the ovarian tissue, the adipose tissue around the ovary was carefully removed. Then, the ovaries were collected in sterile plastic tubes and stored at −80 °C for subsequent analyses.

5.3. Trypsin Digestion and TMT Labeling. Tissue proteins were extracted and digested as previously described.[45] Briefly, frozen tissue samples were weighed (100 mg/mL lysis buffer) and thawed on ice. The samples were resuspended in lysis buffer (30 mM Tris-HCl, 7 M urea, 2 M thiourea, 4% CHAPS; pH 8.5) and incubated on ice for 30 min. The suspensions were sonicated on ice for five cycles consisting of 10 s bursts with a 30 s pause. The lysates were then centrifuged at 12 000 g for 30 min, and the supernatant was filtered with 0.22 μm filters. The filtrate was determined using the BCA Protein Assay kit (Bio-Rad) according to the manufacturer's instructions. Three or four randomly selected ovarian tissue samples were pooled in each group. Protein digestion was performed according to the filter-aided sample preparation (FASP) procedure. Briefly, 200 μg of proteins for each sample was incorporated into 30 μL of DT buffer (4% SDS, 100 mM DTT, 150 mM Tris-HCl pH 8.0). Detergent, DTT, and other low-molecular-weight components were removed by repeated ultrafiltration (Microcon units, 10 kD) using UA buffer (8 M urea, 150 mM Tris-HCl, pH 8.0). Then, 100 μL of iodoacetamide (100 mM IAA in UA buffer) was added to block the reduced cysteine residues, and the samples were incubated in the dark for 30 min. The filters were washed with 100 μL of UA buffer three times and then 100 μL of 25 mM NH_4HCO_3 buffer twice. Finally, the protein suspensions were digested with 4 μg of trypsin (Promega) in 40 μL of 25 mM NH_4HCO_3 buffer overnight at 37 °C. The digested peptides of each sample were desalted on C18 Cartridges (Empore SPE Cartridges C18 (standard density), bed I.D. 7 mm, volume 3 mL, Sigma), concentrated by vacuum centrifugation and reconstituted in 40 μL of 0.1% (v/v) formic acid. A 100 μg peptide mixture of each sample was labeled using TMT reagent according to the manufacturer's instructions (Thermo Scientific). Labeled peptides were then fractionated by a high-pH reversed-phase peptide fractionation kit (Thermo Scientific). The dried peptide mixture was reconstituted and acidified with 0.1% TFA solution and loaded into an equilibrated, high-pH, reversed-phase fractionation spin column. Peptides were combined with hydrophobic resin under aqueous conditions and desalted by washing the column with water and low-speed centrifugation. A step gradient of increasing acetonitrile concentrations in a volatile high-pH elution solution was then applied to the columns to elute the bound peptides into 10 different fractions collected by centrifugation. The collected fractions were desalted on C18 Cartridges (Empore SPE Cartridges C18 (standard density), bed I.D. 7 mm, volume 3 mL, Sigma) and concentrated by vacuum centrifugation.

5.4. LC-MS/MS Analysis. LC-MS/MS analysis was performed using an EASY-nLC 1200 UHPLC system (Thermo Fisher Scientific, San Jose, CA) coupled with a Q Exactive mass spectrometer (Thermo Fisher). The peptides were loaded onto a reversed-phase trap column (Thermo Scientific Acclaim PepMap100, 100 μm × 2 cm, nanoViper C18) connected to the C18 reversed-phase analytical column (Thermo Scientific Easy Column, 10 cm × 75 μm, 3 μm) in buffer A (0.1% formic acid) and separated with a linear gradient of buffer B (84% acetonitrile and 0.1% formic acid) at a flow rate of 300 nL/min controlled by IntelliFlow technology. The mass spectrometer was operated in positive-ion mode. MS data were acquired using a data-dependent top 10 method dynamically choosing the most abundant precursor ions from the survey scan (300−1800 m/z) for HCD fragmentation. The automatic gain control (AGC) target value was 3×10^6, and the maximum ion injection time was 10 ms. The dynamic exclusion duration was 40.0 s. Survey scans were acquired at a resolution of 70 000 at m/z 200, the resolution for HCD spectra was set to 17 500 at m/z 200, and the isolation width was 2 m/z. The normalized collision energy was 30 eV, and the underfill ratio, which specifies the minimum percentage of the target value likely to be reached at maximum fill time, was defined as 0.1%. The instrument was run with peptide recognition mode enabled.

5.5. Database Search. The resulting spectra from each run were searched separately against *Ensemble_Rattus_20210609* using the MASCOT engine (Matrix Science, London, U.K.; version 2.2) embedded into Proteome Discoverer 1.4 software for identification and quantitation analysis. The search parameters were set as follows: the mass tolerance for precursor ions was 20 ppm, and the mass tolerance for product ions was 0.1 Da. A maximum of 2 miscleavage sites was allowed. The identified PSMs and proteins were retained and analyzed with an FDR of no more than 1.0%. The protein ratios are calculated as the median of only unique peptides of the protein. All peptide ratios were normalized by the median protein ratio. The median protein ratio should be 1 after normalization.

5.6. Bioinformatic Analysis of Proteins and DEPs. *5.6.1. Enrichment of Gene Ontology Analysis.* Proteins were classified by GO annotation into three categories, namely,

https://doi.org/10.1021/acsomega.3c00578
ACS Omega 2023, 8, 24831−24840

biological process, cellular compartment, and molecular function. For each category, a two-tailed Fisher's exact test was employed to test the enrichment of the differentially expressed protein against all identified proteins. GO terms with a corrected p value <0.05 were considered significant.[47]

5.6.2. Enrichment of Pathway Analysis. The Kyoto Encyclopedia of Genes and Genomes (KEGG) database was used to identify enriched pathways by a two-tailed Fisher's exact test to test the enrichment of the differentially expressed protein against all identified proteins. The pathways with a corrected p value <0.05 were considered significant. These pathways were classified into hierarchical categories according to the KEGG website.[46] The probable protein−protein interactions were predicted using the STRING-db server.[47]

■ ASSOCIATED CONTENT

Supporting Information

The Supporting Information is available free of charge at https://pubs.acs.org/doi/10.1021/acsomega.3c00578.

Detailed information of protein and peptide quantification of the DEPs (XLSX)

■ AUTHOR INFORMATION

Corresponding Authors

Guimin Zhang − *National Engineering and Technology Research Center of Chirality Pharmaceutical, Lunan Pharmaceutical Group Co. Ltd., Linyi 276006 Shandong, China*; Email: lunanzhangguimin@yeah.net

Jingchun Yao − *State Key Laboratory of Integration and Innovation of Classic Formula and Modern Chinese Medicine, Lunan Pharmaceutical Group Co. Ltd., Linyi 276006 Shandong, China*; Email: yaojingchun@yeah.net

Authors

Jianmei Yang − *Department of Pediatric Endocrinology, Shandong Provincial Hospital affiliated to Shandong First Medical University, Jinan 250021 Shandong, China; State Key Laboratory of Integration and Innovation of Classic Formula and Modern Chinese Medicine, Lunan Pharmaceutical Group Co. Ltd., Linyi 276006 Shandong, China; Department of Pediatric Endocrinology, Shandong Provincial Hospital, Cheeloo College of Medicine, Shandong University, Jinan 250021 Shandong, China*; orcid.org/0000-0002-8017-120X

Enli Wang − *State Key Laboratory of Integration and Innovation of Classic Formula and Modern Chinese Medicine, Lunan Pharmaceutical Group Co. Ltd., Linyi 276006 Shandong, China*

Wenbin Chen − *Scientific Center, Shandong Provincial Hospital affiliated to Shandong First Medical University, Jinan 250021 Shandong, China*

Baihui Xu − *State Key Laboratory of Integration and Innovation of Classic Formula and Modern Chinese Medicine, Lunan Pharmaceutical Group Co. Ltd., Linyi 276006 Shandong, China*

Chen Chen − *Endocrinology, SBMS, Faculty of Medicine, The University of Queensland, St Lucia, QLD 4072, Australia*

Complete contact information is available at: https://pubs.acs.org/10.1021/acsomega.3c00578

Author Contributions

J. Yao and G.Z. conceived and designed the study. E.W. and B.X. raised the animals. J. Yang, W.C., and B.X. conducted the research. J. Yang designed the statistical analyses and wrote the manuscript. C.C. discussed and edited the final version of the manuscript. All authors read and approved the final manuscript.

Notes

The authors declare no competing financial interest.

■ ACKNOWLEDGMENTS

This work was financially supported by the National Natural Science Foundation of China (82100920), Natural Science Foundation of Shandong Province (CN) (ZR2020MH107), China Postdoctoral Science Foundation (2021M691387), and Postdoctoral Creative Funding in Shangdong Province (202103062).

■ REFERENCES

(1) Azziz, R.; Carmina, E.; Chen, Z.; Dunaif, A.; Laven, J. S.; Legro, R. S.; Lizneva, D.; Natterson-Horowtiz, B.; Teede, H. J.; Yildiz, B. O. Polycystic ovary syndrome. *Nat. Rev. Dis. Primers* **2016**, *2*, 16057.

(2) (a) Teede, H. J.; Misso, M. L.; Costello, M. F.; Dokras, A.; Laven, J.; Moran, L.; Piltonen, T.; Norman, R. J.; et al. Recommendations from the international evidence-based guideline for the assessment and management of polycystic ovary syndrome. *Hum. Reprod.* **2018**, *33*, 1602−1618. (b) Wild, R. A. Long-term health consequences of PCOS. *Hum. Reprod. Update* **2002**, *8*, 231−241.

(3) Wang, W.; Jiang, Q.; Niu, Y.; Ding, Q.; Yang, X.; Zheng, Y.; Hao, J.; Wei, D. Proteomics and bioinformatics analysis of follicular fluid from patients with polycystic ovary syndrome. *Front. Mol. Biosci.* **2022**, *9*, No. 956406.

(4) Zhang, Z.; Wu, S.; Stenoien, D. L.; Pasa-Tolic, L. High-throughput proteomics. *Annu. Rev. Anal. Chem.* **2014**, *7*, 427−454.

(5) Sim, Y. J.; Ryu, A. R.; Lee, M. Y. Proteomic analysis of human follicular fluid from polycystic ovary syndrome patients. *Biotechnol. Appl. Biochem.* **2022**, *69*, 289−295.

(6) Wu, L.; Sun, Y.; Wan, J.; Luan, T.; Cheng, Q.; Tan, Y. A proteomic analysis identifies candidate early biomarkers to predict ovarian hyperstimulation syndrome in polycystic ovarian syndrome patients. *Mol. Med. Rep.* **2017**, *16*, 272−280.

(7) Xu, W. L.; Liu, G. Y.; Zhang, N.; Ren, J.; Li, X. Y.; Li, Y. Q.; Chen, Y.; Liu, J. Y. Untargeted metabolomics analysis of serum and follicular fluid samples from women with polycystic ovary syndrome. *Minerva Endocrinol.* **2023**, *48* (2), 160−171.

(8) Shi, Y.; Guo, M.; Yan, J.; Sun, W.; Zhang, X.; Geng, L.; Xu, L.; Chen, Z. Analysis of clinical characteristics in large-scale Chinese women with polycystic ovary syndrome. *Neuro Endocrinol. Lett.* **2007**, *28*, 807−810.

(9) (a) Dahan, M. H.; Reaven, G. Relationship among obesity, insulin resistance, and hyperinsulinemia in the polycystic ovary syndrome. *Endocrine* **2019**, *64*, 685−689. (b) Brassard, M.; AinMelk, Y.; Baillargeon, J. P. Basic infertility including polycystic ovary syndrome. *Med. Clin. North Am.* **2008**, *92*, 1163−1192. (c) Lim, S. S.; Norman, R. J.; Davies, M. J.; Moran, L. J. The effect of obesity on polycystic ovary syndrome: a systematic review and meta-analysis. *Obes. Rev.* **2013**, *14*, 95−109.

(10) (a) Moran, L. J.; Pasquali, R.; Teede, H. J.; Hoeger, K. M.; Norman, R. J. Treatment of obesity in polycystic ovary syndrome: a position statement of the Androgen Excess and Polycystic Ovary Syndrome Society. *Fertil. Steril.* **2009**, *92*, 1966−1982. (b) Teede, H. J.; Misso, M. L.; Deeks, A. A.; Moran, L. J.; Stuckey, B. G.; Wong, J. L.; Norman, R. J.; Costello, M. F.; Guideline Development, G. Assessment and management of polycystic ovary syndrome: summary of an evidence-based guideline. *Med. J. Aust.* **2011**, *195*, S65−S112.

(11) (a) Li, Y.; Chen, C.; Ma, Y.; Xiao, J.; Luo, G.; Li, Y.; Wu, D. Multi-system reproductive metabolic disorder: significance for the

pathogenesis and therapy of polycystic ovary syndrome (PCOS). *Life Sci.* **2019**, *228*, 167−175. (b) Graff, S. K.; Mario, F. M.; Ziegelmann, P.; Spritzer, P. M. Effects of orlistat vs. metformin on weight loss-related clinical variables in women with PCOS: systematic review and meta-analysis. *Int. J. Clin. Pract.* **2016**, *70*, 450−461.

(12) Kumar, P.; Arora, S. Orlistat in polycystic ovarian syndrome reduces weight with improvement in lipid profile and pregnancy rates. *J. Hum. Reprod. Sci.* **2014**, *7*, 255−261.

(13) (a) Panidis, D.; Tziomalos, K.; Papadakis, E.; Chatzis, P.; Kandaraki, E. A.; Tsourdi, E. A.; Katsikis, I. The role of orlistat combined with lifestyle changes in the management of overweight and obese patients with polycystic ovary syndrome. *Clin. Endocrinol.* **2014**, *80*, 432−438. (b) Moini, A.; Kanani, M.; Kashani, L.; Hosseini, R.; Hosseini, L. Effect of orlistat on weight loss, hormonal and metabolic profiles in women with polycystic ovarian syndrome: a randomized double-blind placebo-controlled trial. *Endocrine* **2015**, *49*, 286−289.

(14) Kauffman, A. S.; Thackray, V. G.; Ryan, G. E.; Tolson, K. P.; Glidewell-Kenney, C. A.; Semaan, S. J.; Poling, M. C.; Iwata, N.; Breen, K. M.; Duleba, A. J.; et al. A Novel Letrozole Model Recapitulates Both the Reproductive and Metabolic Phenotypes of Polycystic Ovary Syndrome in Female Mice. *Biol. Reprod.* **2015**, *93*, 69.

(15) Kafali, H.; Iriadam, M.; Ozardali, I.; Demir, N. Letrozole-induced polycystic ovaries in the rat: a new model for cystic ovarian disease. *Arch. Med. Res.* **2004**, *35*, 103−108.

(16) Liu, T.; Liu, D.; Song, X.; Qu, J.; Zheng, X.; Li, J.; Yang, R.; Yang, S.; Zhang, X.; Wang, H.; et al. Lipid Metabolism Was Associated With Oocyte in vitro Maturation in Women With Polycystic Ovarian Syndrome Undergoing Unstimulated Natural Cycle. *Front. Cell Dev. Biol.* **2021**, *9*, No. 719173.

(17) Rajska, A.; Buszewska-Forajta, M.; Rachon, D.; Markuszewski, M. J. Metabolomic Insight into Polycystic Ovary Syndrome-An Overview. *Int. J. Mol. Sci.* **2020**, *21*, No. 4853.

(18) Guijas, C.; Rodriguez, J. P.; Rubio, J. M.; Balboa, M. A.; Balsinde, J. Phospholipase A2 regulation of lipid droplet formation. *Biochim. Biophys. Acta* **2014**, *1841*, 1661−1671.

(19) Balsinde, J.; Winstead, M. V.; Dennis, E. A. Phospholipase A(2) regulation of arachidonic acid mobilization. *FEBS Lett.* **2002**, *531*, 2−6.

(20) Huang, R.; Xue, X.; Li, S.; Wang, Y.; Sun, Y.; Liu, W.; Yin, H.; Tao, T. Alterations of polyunsaturated fatty acid metabolism in ovarian tissues of polycystic ovary syndrome rats. *J. Cell. Mol. Med.* **2018**, *22*, 3388−3396.

(21) Oner, G.; Muderris, I. I. Efficacy of omega-3 in the treatment of polycystic ovary syndrome. *J. Obstet. Gynaecol.* **2013**, *33*, 289−291.

(22) Tithof, P. K.; Roberts, M. P.; Guan, W.; Elgayyar, M.; Godkin, J. D. Distinct phospholipase A2 enzymes regulate prostaglandin E2 and F2alpha production by bovine endometrial epithelial cells. *Reprod. Biol. Endocrinol.* **2007**, *5*, 16.

(23) Karim, S. M. M.; Hillier, K. Prostaglandins in the control of animal and human reproduction. *Br. Med. Bull.* **1979**, *35*, 173−180.

(24) Uyama, T.; Tsuboi, K.; Ueda, N. An involvement of phospholipase A/acyltransferase family proteins in peroxisome regulation and plasmalogen metabolism. *FEBS Lett.* **2017**, *591*, 2745−2760.

(25) Hummasti, S.; Hong, C.; Bensinger, S. J.; Tontonoz, P. HRASLS3 is a PPARgamma-selective target gene that promotes adipocyte differentiation. *J. Lipid Res.* **2008**, *49*, 2535−2544.

(26) Jaworski, K.; Ahmadian, M.; Duncan, R. E.; Sarkadi-Nagy, E.; Varady, K. A.; Hellerstein, M. K.; Lee, H. Y.; Samuel, V. T.; Shulman, G. I.; Kim, K. H.; et al. AdPLA ablation increases lipolysis and prevents obesity induced by high-fat feeding or leptin deficiency. *Nat. Med.* **2009**, *15*, 159−168.

(27) Volat, F. E.; Pointud, J. C.; Pastel, E.; Morio, B.; Sion, B.; Hamard, G.; Guichardant, M.; Colas, R.; Lefrancois-Martinez, A. M.; Martinez, A. Depressed levels of prostaglandin F2alpha in mice lacking Akr1b7 increase basal adiposity and predispose to diet-induced obesity. *Diabetes* **2012**, *61*, 2796−2806.

(28) Feng, Y.; Qi, J.; Xue, X.; Li, X.; Liao, Y.; Sun, Y.; Tao, Y.; Yin, H.; Liu, W.; Li, S.; Huang, R. Follicular free fatty acid metabolic signatures and their effects on oocyte competence in non-obese PCOS patients. *Reproduction* **2022**, *164*, 1−8.

(29) Seery, L. T.; Nestor, P. V.; FitzGerald, G. A. Molecular evolution of the aldo-keto reductase gene superfamily. *J. Mol. Evol.* **1998**, *46*, 139−146.

(30) Jin, Y.; Penning, T. M. Aldo-keto reductases and bioactivation/detoxication. *Annu. Rev. Pharmacol. Toxicol.* **2007**, *47*, 263−292.

(31) Lau, E. T.; Cao, D.; Lin, C.; Chung, S. K.; Chung, S. S. Tissue-specific expression of two aldose reductase-like genes in mice: abundant expression of mouse vas deferens protein and fibroblast growth factor-regulated protein in the adrenal gland. *Biochem. J.* **1995**, *312*, 609−615.

(32) Tirard, J.; Gout, J.; Lefrancois-Martinez, A. M.; Martinez, A.; Begeot, M.; Naville, D. A novel inhibitory protein in adipose tissue, the aldo-keto reductase AKR1B7: its role in adipogenesis. *Endocrinology* **2007**, *148*, 1996−2005.

(33) Ge, X.; Yin, L.; Ma, H.; Li, T.; Chiang, J. Y.; Zhang, Y. Aldo-keto reductase 1B7 is a target gene of FXR and regulates lipid and glucose homeostasis. *J. Lipid Res.* **2011**, *52*, 1561−1568.

(34) Brockstedt, E.; Peters-Kottig, M.; Badock, V.; Hegele-Hartung, C.; Lessl, M. Luteinizing hormone induces mouse vas deferens protein expression in the murine ovary. *Endocrinology* **2000**, *141*, 2574−2581.

(35) Baumann, C.; Davies, B.; Peters, M.; Kaufmann-Reiche, U.; Lessl, M.; Theuring, F. AKR1B7 (mouse vas deferens protein) is dispensable for mouse development and reproductive success. *Reproduction* **2007**, *134*, 97−109.

(36) Guo, Y.; Qi, Y.; Yang, X.; Zhao, L.; Wen, S.; Liu, Y.; Tang, L. Association between Polycystic Ovary Syndrome and Gut Microbiota. *PLoS One* **2016**, *11*, No. e0153196.

(37) Wu, Y. X.; Yang, X. Y.; Han, B. S.; Hu, Y. Y.; An, T.; Lv, B. H.; Lian, J.; Wang, T. Y.; Bao, X. L.; Gao, L.; et al. Naringenin regulates gut microbiota and SIRT1/ PGC-1a signaling pathway in rats with letrozole-induced polycystic ovary syndrome. *Biomed. Pharmacother.* **2022**, *153*, No. 113286.

(38) (a) Li, L.; Zhang, J.; Deng, Q.; Li, J.; Li, Z.; Xiao, Y.; Hu, S.; Li, T.; Tan, Q.; Li, X.; et al. Proteomic Profiling for Identification of Novel Biomarkers Differentially Expressed in Human Ovaries from Polycystic Ovary Syndrome Patients. *PLoS One* **2016**, *11*, No. e0164538. (b) González, F.; Considine, R. V.; Abdelhadi, O. A.; Acton, A. J. Saturated Fat Ingestion Promotes Lipopolysaccharide-Mediated Inflammation and Insulin Resistance in Polycystic Ovary Syndrome. *J. Clin. Endocrinol. Metab.* **2019**, *104*, 934−946. (c) Liu, Y.; Liu, H.; Li, Z.; Fan, H.; Yan, X.; Liu, X.; Xuan, J.; Feng, D.; Wei, X. The Release of Peripheral Immune Inflammatory Cytokines Promote an Inflammatory Cascade in PCOS Patients via Altering the Follicular Microenvironment. *Front. Immunol.* **2021**, *12*, 685724.

(39) Hu, C.; Pang, B.; Ma, Z.; Yi, H. Immunophenotypic Profiles in Polycystic Ovary Syndrome. *Mediators Inflamm.* **2020**, *2020*, No. 5894768.

(40) Zhu, Q.; Zhou, H.; Zhang, A.; Gao, R.; Yang, S.; Zhao, C.; Wang, Y.; Hu, J.; Goswami, R.; Gong, L.; Li, Q. Serum LBP Is Associated with Insulin Resistance in Women with PCOS. *PLoS One* **2016**, *11*, No. e0145337.

(41) (a) Yang, S.; Li, Q.; Song, Y.; Tian, B.; Cheng, Q.; Qing, H.; Zhong, L.; Xia, W. Serum complement C3 has a stronger association with insulin resistance than high-sensitivity C-reactive protein in women with polycystic ovary syndrome. *Fertil. Steril.* **2011**, *95*, 1749−1753. (b) Kaya, C.; Pabuccu, R.; Berker, B.; Satiroglu, H. Plasma interleukin-18 levels are increased in the polycystic ovary syndrome: relationship of carotid intima-media wall thickness and cardiovascular risk factors. *Fertil. Steril.* **2010**, *93*, 1200−1207.

(42) Banaszewska, B.; Siakowska, M.; Chudzicka-Strugala, I.; Chang, R. J.; Pawelczyk, L.; Zwozdziak, B.; Spaczynski, R.; Duleba, A. J. Elevation of markers of endotoxemia in women with polycystic ovary syndrome. *Hum. Reprod.* **2020**, *35*, 2303−2311.

https://doi.org/10.1021/acsomega.3c00578
ACS Omega 2023, 8, 24831−24840

(43) Zou, Z. Y.; Hu, Y. R.; Ma, H.; Wang, Y. Z.; He, K.; Xia, S.; Wu, H.; Xue, D. F.; Li, X. G.; Ye, X. L. Coptisine attenuates obesity-related inflammation through LPS/TLR-4-mediated signaling pathway in Syrian golden hamsters. *Fitoterapia* **2015**, *105*, 139−146.
(44) Lucas, N.; Legrand, R.; Deroissart, C.; Dominique, M.; Azhar, S.; Le Solliec, M. A.; Leon, F.; do Rego, J. C.; Dechelotte, P.; Fetissov, S. O.; Lambert, G. Hafnia alvei HA4597 Strain Reduces Food Intake and Body Weight Gain and Improves Body Composition, Glucose, and Lipid Metabolism in a Mouse Model of Hyperphagic Obesity. *Microorganisms* **2020**, *8*, No. 35.
(45) Wang, H.; Qian, W. J.; Chin, M. H.; Petyuk, V. A.; Barry, R. C.; Liu, T.; Gritsenko, M. A.; Mottaz, H. M.; Moore, R. J.; Camp Ii, D. G.; et al. Characterization of the mouse brain proteome using global proteomic analysis complemented with cysteinyl-peptide enrichment. *J. Proteome Res.* **2006**, *5*, 361−369.
(46) Huang, D. W.; Sherman, B. T.; Lempicki, R. A. Bioinformatics enrichment tools: paths toward the comprehensive functional analysis of large gene lists. *Nucleic Acids Res.* **2009**, *37*, 1−13.
(47) Franceschini, A.; Szklarczyk, D.; Frankild, S.; Kuhn, M.; Simonovic, M.; Roth, A.; Lin, J.; Minguez, P.; Bork, P.; von Mering, C.; Jensen, L. J. STRING v9.1: protein-protein interaction networks, with increased coverage and integration. *Nucleic Acids Res.* **2012**, *41*, D808−D815.

https://doi.org/10.1021/acsomega.3c00578
ACS Omega 2023, 8, 24831−24840